Microwave dielectric constant of liquid hydrocarbons: Application to the depth estimation of Titan's lakes

Philippe Paillou, K. L. Mitchell, Stephen D. Wall, Gilles Ruffié, C. Wood, R. D. Lorenz, Ellen R. Stofan, J.I. Lunine, R. Lopes, P. Encrenaz

Microwave dielectric constant of liquid hydrocarbons: Application to the depth estimation of Titan's lakes

Philippe Paillou[1], Karl Mitchell[2], Stephen Wall[2], Gilles Ruffié[3], Charles Wood[4], Ralph Lorenz[5], Ellen Stofan[6], Jonathan Lunine[7], Rosaly Lopes[2], Pierre Encrenaz[8]

[1]OASU, UMR 5804, Floirac, France, [2]JPL, Pasadena, CA, USA, [3]IMS, UMR 5218, Pessac, France, [4]Planetary Science Institute, Tucson, AZ, USA, [5]Johns Hopkins University APL, Laurel, MD, USA, [6]Proxemy Research, Rectortown, VA, USA, [7]Lunar and Planetary Laboratory, Tucson, AZ, USA, [8]Observatoire de Paris, LERMA, Paris, France

Cassini RADAR reveals the surface of Titan since flyby Ta acquired on October 2004. The RADAR instrument discovered volcanic structures, craters, dunes, channels, lakes and seas. In particular, flyby T16 realized in July 2006 imaged tens of radar-dark features close to Titan's north pole. They are interpreted as lakes filled with liquid hydrocarbons – mainly methane, a key material in the geologic and climatic history of Titan. In order to perform quantitative analysis and modeling of the radar response of Titan's lakes, the dielectric constant of liquid hydrocarbons is a crucial parameter, in particular to estimate the radar wave attenuation. We present here first measurements of the dielectric constant of LNG (Liquefied Natural Gas), mainly composed of methane, at Ku-band (10 – 13 GHz): we obtained a value $\varepsilon = 1.75 - 0.002j$. This value is used to model the radar backscattering of lakes observed during T16 flyby. Using a two-layer scattering model, we derive a relationship that is used to estimate a minimum depth for Titan's lakes. The proposed relationship is also coherent with the observation that the larger and then the deeper lakes are also the darker in radar images.

1. Introduction

Titan, the second satellite in size in the solar system, is also the only moon with a thick atmosphere. Titan is a principal scientific objective of the Cassini-Huygens mission which has been in orbit around Saturn since July 2004. The RADAR instrument [Elachi et al., 2004] is a high frequency Ku-band (13.78 GHz – 2.18 cm) radar, which is able to image Titan's surface through its atmosphere. The SAR (Synthetic Aperture Radar) mode allows the instrument to map the surface of Titan with a spatial resolution as high as 350 m. Several flybys over Titan have been performed by the Cassini spacecraft: they revealed a very geologically diverse and young surface, with dome-like volcanic constructs, flows and sinuous channels, dunes, lakes and seas [Elachi et al., 2005; Elachi et al., 2006; Lorenz et al., 2006a; Lorenz et al., 2006b; Lopes et al., 2007; Radebaugh et al., 2007].

The Titan flyby on 22 July 2006, known as T16, revealed the first extra-terrestrial lakes [Stofan et al., 2007]. A 6130 km long SAR swath, from mid-northern latitudes to near the North pole, imaged more than 75 radar-dark patches, from 3 km to more than 70 km in size (see Figure 1 and Table 1). The low radar backscattering of these dark structures is consistent with a smooth surface filled with a low dielectric constant material. Also, one can observe at several radar-dark patches, radar-dark sinuous features, interpreted as channels, which lead into the dark patch. Several dark patches are also steep-sided circular depressions, resembling terrestrial lakes located within volcanic calderas or karst sinkholes. Considering the morphology of T16 radar-dark patches and that liquid methane and ethane are expected to be abundant and stable on the surface of Titan near the poles [Lunine et al., 1983; Rannou et al., 2006; Tobie et al., 2006; Mitri et al., 2007], Stofan et al. (2007) conclude that these dark structures are lakes containing liquid hydrocarbons. The exact composition of this liquid is still unknown, but it is considered to be mainly methane and/or ethane probably containing dissolved nitrogen [Mitri et al., 2007]. Several depressions however present a brighter radar return and might be only partly filled, if not dried-out. Some lakes also present increased radar brightness near their edge, which might be due to a reflection from the lake bottom, in the case it is shallow enough so that the

bottom signal is not completely attenuated. Changes in σ_0 are unlikely to be caused by a wind effect roughening the lake's surface, as tidal winds at high latitudes are predicted to be an order of magnitude lower than that needed to form capillary waves in liquid hydrocarbons [Lorenz et al., 2005].

In order to quantitatively model the radar response over Titan's lakes, a key parameter is needed: the dielectric constant of liquid hydrocarbons, in particular liquid methane. This parameter controls the attenuation (and then penetration depth) of the radar wave, and also the reflectivity of the liquid surface. Few references provide dielectric constant of liquid hydrocarbons at Ku-band, and no measurement for liquid methane is available: estimates range from 1.5 to 2.0 for the real part of the dielectric constant, while the loss tangent is considered to be in the 10^{-3} – 10^{-5} range [Thompson and Squyres, 1990; Sen et al., 1992]. Such an uncertainty, especially for the loss tangent, yields difficulties in estimating radar penetration depth and reflectivity over liquid methane. We present here first measurements of the dielectric constant of LNG (Liquefied Natural Gas), mainly composed of methane, at Ku-band. The obtained value is used to model the radar backscattering of lakes observed during the T16 flyby, in order to derive a relationship that can be used to estimate a minimum depth for Titan's lakes.

2. Measurements of the Dielectric Constant of LNG

Instead of considering pure liquid methane, which is hard to manipulate in a laboratory environment, we used Liquefied Natural Gas, i.e. natural gas that has been liquefied at low temperature (–163 ^{o}C) for transport and storage. Gaz de France produces, stores and distributes purified LNG which contains more than 90% pure methane, the remaining 10% being a mixture of nitrogen and heavier hydrocarbons. LNG might then be a very good terrestrial analog to the liquid filling Titan's lakes. We had access to the gas terminal in Montoir de Bretagne that is operated by Gaz de France, and performed measurements on LNG on the site.

We used a free-space method [Ghodgaonkar et al., 1989] to measure the dielectric constant of LNG. Our system consisted of a set of two focused elliptical antennas (10 – 13 GHz frequency range), one being used as an emitter and the other as a receptor. A polystyrene box (of dielectric constant close to the one of air) of known dimensions was placed at the focal point between the two antennas, and filled with the liquid to be measured. Vector network analyzers ANRITSU 37325A and AGILENT E8364B were used as source generator and receptor. A first measurement was performed on the empty polystyrene box in order to measure system losses and perform calibration. We then filled the box with LNG and performed a second measurement (see Figure 2 top). We measured both reflection and transmission coefficients, which allowed us to compute the real part and imaginary parts of the dielectric constant of the material. We initially performed several outdoor experiments using liquid nitrogen in order to test our set-up: we obtained a permittivity of 1.45 and a loss tangent of 10^{-4} at 10 GHz, consistent with previous measurements [Smith et al., 1991]. We estimate the measurement error to about 10% on both the real and imaginary parts of the dielectric constant.

We performed four measurements on the same LNG sample (the polystyrene box was emptied and re-filled each time), which composition was 90% methane, 5% nitrogen and 5% other hydrocarbons (mainly ethane and propane). We obtained an average dielectric constant $\varepsilon = 1.75 - 0.002j$, that is a loss tangent of $1.14\ 10^{-3}$ at a frequency of 13 GHz, close to the upper limit proposed by [Sen et al., 1992], but higher than the $5\ 10^{-4}$ value measured by [Whiffen, 1950] for other liquid hydrocarbons. However, Whiffen (1950) made measurements at room temperature, and loss tangent of liquid hydrocarbons increases with declining temperature. It should also be noted that the loss tangent of pure liquid methane is likely to be lower than the measured value, since our LNG sample contains 5% of heavier hydrocarbons, which dielectric constant is known to be somewhat higher. Our measured value corresponds to a skin depth (*1/e* attenuation depth, see [Ulaby et al., 1982]) of 2.2 m at the 13.78 GHz frequency of the RADAR instrument, meaning that Cassini RADAR should be able to probe through meters of the liquid filling Titan's lakes.

3. Modeling the Radar Backscattering of Titan Lakes

We used the T16 lake list in Table 1 and a simple two-layer scattering model to reproduce observed σ_0 values. Each lake was modeled as a superficial smooth top layer of liquid methane of thickness *d*, which covers a rougher bottom layer made of tholin-like materials. The top layer is characterized by its dielectric constant ($\varepsilon_1 = 1.75 - 0.002j$) and surface roughness (height standard deviation σ_1, correlation length L_1). The bottom layer is also characterized by its dielectric constant ($\varepsilon_2 = 2.20 - 0.01j$, see [Rodriguez et al., 2003]) and roughness (σ_2, L_2). This two-layer model is illuminated by a radar wave of wavelength λ_0 arriving with an incidence angle θ. In order to take into account various surface roughness conditions (from very smooth to very rough surfaces compared to the radar wavelength), we used different backscattering models: IEM (Integral Equation Model) [Fung et al. 1992], PO (Physical Optics) model [Ulaby et al., 1982] and GO (Geometric Optics) model [Fung and Eom, 1981]. The complete description of the two-layer scattering model can be found in [Paillou et al., 2006]. The total backscattered power σ_0 for a given lake is then the sum of a surface scattering term (scattering from the liquid methane surface, we did not take into account volume scattering by heterogeneities or suspensions in the liquid) and a sub-surface scattering term (scattering from the lake's bottom, attenuated by a two-way path through the liquid). We considered here a "no wind" hypothesis, i.e. changes in σ_0 are only due to changes in lake depth: darkest lakes are the deepest (only a weak return from the smooth liquid methane surface, the bottom contribution being completely attenuated by the thick liquid layer), and brightest lakes are dry (strong return from the rough open-air bottom).

In order to calibrate our model, we derived roughness parameters (σ, L) of the two layers from two extreme scattering cases observed in Table 1. Darkest lakes (σ_0 lower than –25 dB) were considered to be very deep lakes, for which the backscattering of the upper liquid layer is prevailing on the bottom. They were then used to derive typical roughness parameters of the smooth liquid surface (IEM used): $\sigma_1 = 0.15$ cm and $L_1 = 1.40$ cm for a mean incidence angle of 33^o yields a σ_0 value of –26.8 dB. The brightest lakes (σ_0 higher than –11 dB) were considered to be dry lakes, i.e. all the backscattered power

is from the rough tholin-material bottom. They were used to estimate the roughness parameters of the rougher lake bottom (GO model used): σ_2 = 2.0 cm and L_2 = 6.0 cm for a mean incidence angle of 33° yields a σ_0 value of –11.8 dB. Eventually, a range of roughness parameter and incidence angle values should be considered in order to produce more complete simulation results, but we are here mainly interested into first order results to constrain the depth of Titan's lakes.

4. Lakes Depth Estimation

Using previously fixed parameters in our two-layer scattering model, we computed theoretical σ_0 values for a varying thickness of the liquid filling the lakes. The obtained σ_0 – depth relationship is presented in Figure 2 bottom for an incidence angle θ = 28, 33, 38°. The incidence angle mainly controls the "saturation level" of σ_0: lower incidence angle leads to a higher backscattering level of dark lakes. We also show in Figure 2 bottom the σ_0 – depth relationship for a liquid with a lower loss tangent ($5\ 10^{-4}$) in order to illustrate the importance of this parameter (the lower the loss tangent, the deeper Radar can see). We shall consider in the following a mean incidence angle of 33° (see Table 1): for a detection limit of about –27 dB, the RADAR instrument is likely to see through 7 m of liquid methane. Figure 3 top presents the σ_0 distribution for the 77 lakes in Table 1. Two main groups can be distinguished: 1) "bright lakes" with σ_0 higher than –19 dB, which correspond to a depth lower than 2 m; 2) "dark lakes" with σ_0 lower than –22 dB, which correspond to a depth higher than 3 m (see curve θ = 33° in Figure 2 bottom). The limit between bright (i.e. shallow) and dark (i.e. deep) lakes lies around –19/–22 dB. This transition between bright and dark lakes can also be seen in Figure 3 bottom, which plots the lake area in km^2 versus σ_0: bright lakes (σ_0 higher than –19 dB) correspond to small lakes with an area lower than 50 km^2, while dark lakes (σ_0 lower than –22 dB) correspond to larger lakes with an area higher than 100 km^2. Considering our model results and geomorphological evidences from terrestrial lakes, it is reasonable to assume that the bigger (and darker) lakes are deeper, while the smaller (and brighter) ones are shallower. This observation also supports the "no wind" and "liquid

filled" assumptions: in a windy context, one would expect the larger lakes to be the more likely to have ripples and waves, causing roughening and thus radar brightening.

The proposed σ_0 – depth relationship, although based on a simple scattering model and on a "no wind" hypothesis, can however be used to obtain first order estimates for the lower limits of hydrocarbon volume contained in lakes [Lorenz et al., 2007]: for instance, lake #66 is at least 4 m deep and has an area of 250 km^2, so it should contain a minimum volume of 1 km^3 of liquid hydrocarbons. Finally, one can observe in Figure 2 bottom that σ_0 presents a strong variation (more than 15 dB) for a rather small change in lake depth for shallow lakes (less than 5 m). This high sensitivity of the radar signal can be used to detect meter-scale level changes of Titan's lakes: monitoring of tide effect [Lorenz et al., 2003] and seasonal changes by evaporation [Mitri et al., 2007] for instance, when repeated SAR coverage of the North polar regions will be available.

Acknowledgments

The authors are grateful to Gaz de France (L. Duquesne, A. Le Cloarec, A. Peigné, Ph. Loisel) for giving access to its LNG facilities in Montoir de Bretagne, and to Agilent Technologies (E. Chollier, D. Ferret) for providing E8364B VNA.

References

Elachi, Ch., et al., "RADAR: The Cassini Titan Radar Mapper", *Space Science Reviews*, vol. 115, pp. 71-110, 2004.

Elachi, Ch., et al., "Cassini Radar views the surface of Titan", *Science*, vol. 308, pp. 970-974, 2005.

Elachi, Ch., et al., "Titan Radar mapper observations for Cassini T3 flyby", *Nature*, vol. 441, pp. 709-713, 2006.

Fung, A.K., H.J. Eom, "Multiple Scattering and Depolarization by a Randomly Rough Kirchhoff Surface", *IEEE Transactions on Antennas Propagation*, vol. AP-29, no. 3, pp. 463-471, 1981.

Fung, A.K., Z. Li, K.S. Chen, "Backscattering from a randomly rough dielectric surface", *IEEE Trans. Geosci. Remote Sensing*, vol. 30, no. 2, pp. 356-369, 1992.

Ghodgaonkar, D.K., V.V. Varadan, V.K. Varadan, "A free-space method for measurement of dielectric constants and loss tangents at microwave frequencies", *IEEE Trans. Instr. Meas.*, vol. 38, no. 3, pp. 789-796, 1989.

Lopes, R.M.C., et al., "Cryovolcanic Features on Titan's Surface as Revealed by the Cassini Titan Radar Mapper", *Icarus,* vol. 186, pp. 395-412, 2007.

Lorenz, R.D., et al., "The seas of Titan", *EOS*, vol. 84, no 14, pp. 125, 131-132, 2003.

Lorenz, R.D., et al., "Sea-surface wave growth under extraterrestrial atmospheres: Preliminary wind tunnel experiments with application to Mars and Titan", *Icarus*, vol. 175, pp. 556-560, 2005.

Lorenz, R.D., et al., "Titan's young surface: Initial impact crater survey by Cassini RADAR and model comparison", *Geophys. Res. Lett.*, vol. 34, L07204, doi:10.1029/2006GL028971, 2006a.

Lorenz, R.D., et al., "The sand seas of Titan: Cassini RADAR observations of longitudinal dunes", *Science*, vol. 312, pp. 724-727, 2006b.

Lorenz, R.D., et al., "Titan's inventory of organic surface material", *Geophys. Res. Lett.*, 2007, in press.

Lunine, J.I., D.J. Stevenson, Y.L. Yung, "Ethane oceans on Titan", *Science*, vol. 222, pp. 1229-1230, 1983.

Mitri, G., A.P. Showman, J.I. Lunine, R.D. Lorenz, "Hydrocarbon lakes on Titan", *Icarus*, vol. 186, no. 1, pp. 385-394, 2007.

Paillou, Ph., M. Crapeau, Ch. Elachi, S. Wall, P. Encrenaz, "Models of SAR backscattering for bright flows and dark spots on Titan", *Journal of Geophysical Research*, vol. 111, E11011, doi: 10.1029/2006JE002724, 2006.

Radebaugh, J., et al., "Mountains on Titan Observed by Cassini RADAR", *Icarus*, vol. 192, pp. 77-91, 2007.

Rannou, P., "The latidunal distribution of clouds on Titan", *Science*, vol. 311, pp. 201-205, 2006.

Rodriguez, S., Ph. Paillou, et al., “Impact of tholins present in Titan’s atmosphere on the Cassini radar experiment”, *Icarus*, vol. 164, pp. 213-227, 2003.

Sen, A.D., et al., “Dielectric constant of liquid alkanes and hydrocarbon mixtures”, *J. Appl. Phys.*, vol. 25, pp. 516-512, 1992.

Smith, P.A., et al., “The dielectric loss tangent of liquid nitrogen”, *Supercond. Sci. Technol.*, vol. 4, pp. 128-129, 1991.

Stofan, E.R., et al., “The lakes of Titan”, *Nature*, vol. 445, pp. 61-64, 2007.

Thompson, W.R., S.W. Squyres, “Titan and other icy satellites: Dielectric properties of constituent materials and implications for radar sounding”, *Icarus*, vol. 86, pp. 336-354, 1990.

Tobie, G., J.I. Lunine, Ch. Sotin, “Episodic outgassing as the origin of atmospheric methane on Titan”, *Nature*, vol. 440, pp. 61-64, 2006.

Ulaby, F.T., R.K. Moore, A.K. Fung, *Microwave Remote Sensing: Active and Passive*, vol. 2, Norwood MA, Artech House, 1982.

Whiffen, D.H., “Measurements on the absorption of microwaves. Part IV: non-polar liquids”, *Trans. Faraday Soc.*, vol. 46, pp. 124-130, 1950.

ID	S0	IA	AR	LAT	LON	ID	S0	IA	AR	LAT	LON
1	-23.13	24.27	13.50	71.17	134.48	40	-22.37	34.58	113.95	81.20	53.41
2	-13.51	25.55	13.50	72.00	132.58	41	-15.69	31.18	59.01	82.09	48.63
3	-10.72	30.52	29.43	71.43	126.46	42	-15.93	39.48	13.50	79.35	49.41
4	-12.27	29.06	8.85	71.87	128.54	43	-14.88	38.76	13.50	79.38	48.14
5	-14.12	26.70	3.70	72.60	130.41	44	-14.14	37.43	16.13	80.00	48.05
6	-12.81	30.25	76.59	71.89	126.36	45	-14.27	31.15	21.34	82.13	42.29
7	-12.48	31.32	3.70	72.60	124.81	46	-13.45	32.68	64.58	81.64	41.17
8	-13.67	31.20	1.50	73.12	124.00	47	-14.58	33.64	79.65	80.77	42.09
9	-15.55	29.67	6.89	73.65	125.35	48	-29.47	32.08	312.40	81.68	37.70
10	-12.21	25.69	46.45	74.18	130.18	49	-22.21	36.97	197.86	79.92	39.53
11	-18.65	34.97	13.50	72.82	119.31	50	-15.24	33.21	29.43	79.55	26.68
12	-16.52	28.14	6.89	74.22	126.00	51	-28.34	36.47	76.59	78.72	29.69
13	-9.80	29.45	6.89	74.39	124.57	52	-14.96	38.16	13.50	77.83	28.70
14	-16.75	26.66	19.14	74.68	126.20	53	-17.88	39.52	7.80	77.30	28.74
15	-14.17	26.77	48.41	75.34	125.08	54	-14.92	33.76	13.50	78.90	23.28
16	-14.71	33.37	3.70	74.01	119.05	55	-12.99	32.47	29.43	79.24	21.61
17	-14.18	33.44	3.58	74.16	118.81	56	-25.12	39.16	64.58	76.96	25.73
18	-13.59	33.98	0.76	74.14	118.07	57	-13.56	34.41	51.48	78.23	20.56
19	-13.99	35.70	12.40	74.28	115.06	58	-15.75	37.52	3.70	77.01	23.20
20	-13.97	31.02	18.03	78.20	112.46	59	-18.87	30.95	145.31	78.53	16.37
21	-13.05	37.04	237.28	76.93	104.80	60	-24.03	35.26	142.13	76.65	20.44
22	-11.21	34.52	8.72	80.69	87.14	61	-19.40	38.91	51.48	75.18	18.44
23	-11.05	34.23	3.70	80.86	86.43	62	-22.31	38.13	12.34	75.22	17.28
24	-9.89	33.62	0.76	81.09	85.47	63	-15.48	35.20	3.70	75.90	14.82
25	-13.26	33.32	26.36	81.24	85.32	64	-15.78	35.16	6.76	76.00	14.22
26	-9.85	32.69	11.05	81.35	84.92	65	-16.74	37.88	29.43	74.79	17.33
27	-11.01	31.76	29.43	81.52	86.98	66	-24.19	31.00	250.54	76.67	10.85
28	-12.48	35.26	3.70	80.58	83.86	67	-14.56	36.32	25.75	73.72	10.14
29	-11.51	30.86	19.26	82.27	85.79	68	-15.84	36.18	13.50	71.25	7.00
30	-17.57	31.37	13.50	82.07	84.07	69	-13.27	34.65	8.85	71.26	5.68
31	-11.40	35.24	7.56	80.63	82.17	70	-9.80	32.02	10.44	71.90	3.18
32	-12.73	34.77	8.85	80.90	80.72	71	-9.70	30.86	13.50	70.77	0.87
33	-12.52	36.14	29.43	80.67	79.56	72	-13.96	36.61	10.93	69.56	5.66
34	-13.67	35.39	37.51	80.45	76.90	73	-11.57	33.44	38.92	68.49	1.96
35	-12.50	32.48	19.93	82.04	76.92	74	-8.40	29.17	103.54	67.49	357.88
36	-25.30	31.31	225.73	82.13	74.06	75	-10.03	30.58	51.48	65.85	354.79
37	-14.59	34.10	37.02	81.68	68.31	76	-10.03	28.57	64.03	65.14	354.23
38	-14.76	38.40	13.50	80.07	62.28	77	-9.23	38.63	51.48	78.29	34.26
39	-17.32	31.55	32.79	82.42	56.50						

Table 1. T16 lakes (ID: lake number, S0: average σ_0 in dB, IA: radar incidence angle in degrees, AR: lake area in km^2, LAT: center latitude in degrees, LON: center longitude in degrees).

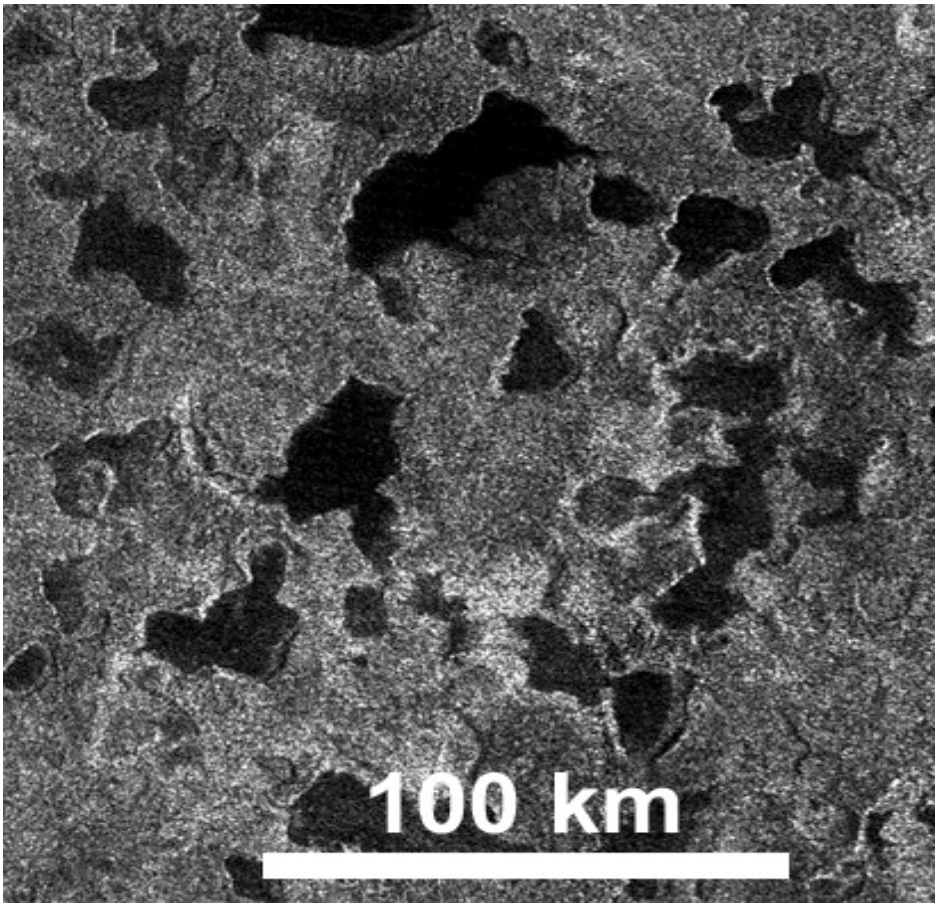

Figure 1. Extract of T16 SAR swath showing dark patches interpreted as lakes containing liquid hydrocarbons.

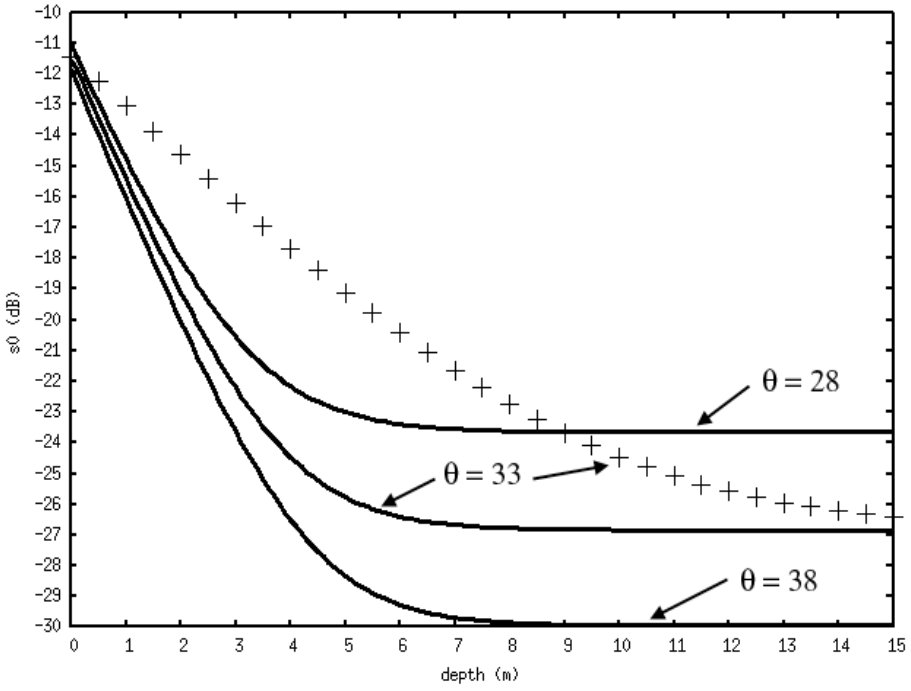

Figure 2. *Top:* Poring LNG in the polystyrene box. Emitting and receiving antennas allow to measure the dielectric constant in the 10 – 13 GHz frequency range. *Bottom:* Total SAR backscattered power versus lake depth at an incidence angle of 28°, 33° and 38°. Plain lines correspond to a loss tangent of 1.14 10^{-3}, while dot line corresponds to a loss tangent of 5 10^{-4}.

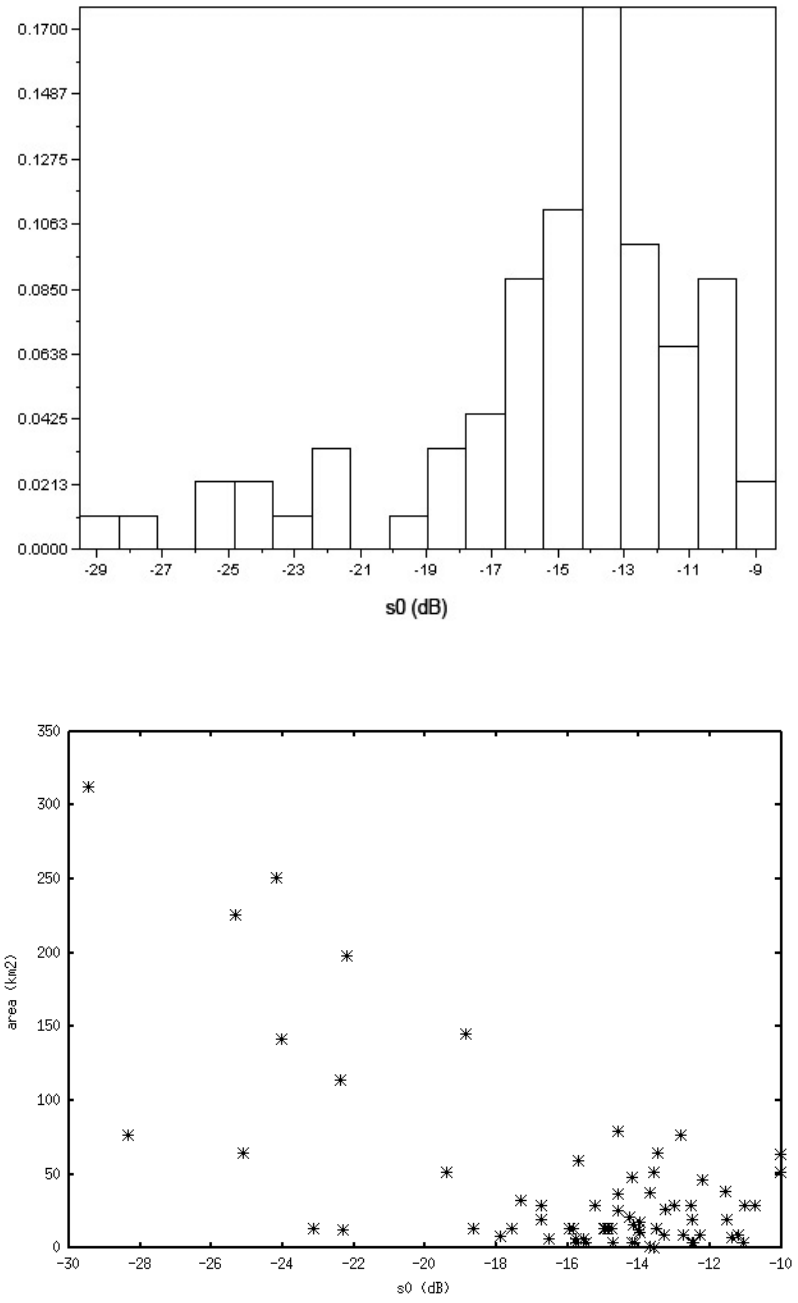

Figure 3. *Top:* Histogram of σ_0 distribution for the 77 lakes, showing two main groups: "bright lakes" with σ_0 higher than –19 dB and "dark lakes" with σ_0 lower than –22 dB. *Bottom:* Plot of T16 lake area (in km^2) versus mean σ_0 (in dB): smaller lakes are also the brightest, while larger ones are the darkest, with a limit between the two groups around –19/–22 dB.